N90-19440

TDA Progress Report 42-99

November 15, 1989

Performance of the All-Digital Data-Transition Tracking Loop in the Advanced Receiver

U. Cheng and S. Hinedi
Communications Systems Research Section

This article describes the performance of the all-digital data-transition tracking loop (DTTL) with coherent or noncoherent sampling. The effects of few samples per symbol and of noncommensurate sampling rates and symbol rates are addressed and analyzed. Their impacts on the loop phase-error variance and the mean time to lose lock (MTLL) are quantified through computer simulations. The analysis and preliminary simulations indicate that with three to four samples per symbol, the DTTL can track with negligible jitter because of the presence of Earth Doppler rate. Furthermore, the MTLL is also expected to be large enough to maintain lock over a Deep Space Network track.

I. Introduction

In modern digital communication systems, analog-to-digital conversion (ADC) is performed as far toward the front end as possible using available technology. Usually, the received signal is amplified and then downconverted to the appropriate frequency for digital conversion. Thereafter, various system functions are performed digitally, including carrier, subcarrier, and symbol synchronization, as well as signal detection and decoding. Depending on the application, either the baseband signals (inphase and quadrature) or the intermediate frequency (IF) signal can be sampled. Furthermore, the sampling clock can be free-running or controlled by the symbol-synchronization loop. In the latter case, the sampling clock can be adjusted to obtain an integer number of samples per cycle of the IF signal, or to obtain an integer number of samples per received symbol. All of these issues affect the final architecture and design of a receiver and influence the amount of cross-coupling among the various loops.

Since sampling is done up front, the various tracking loops need to be implemented digitally. The classical analog integrate-and-dump (I&D) filters, which are typically part of the loop arms (inphase and quadrature), must be replaced by digital accumulators. This article investigates the performance of the all-digital data-transition tracking loop (DTTL) with small noninteger numbers of samples per symbol. In the previous version of the Advanced Receiver (ARX I) [1], the sampling was performed synchronously with the symbol rate, and a large number of samples per symbol were available. In the current version of the Advanced Receiver (ARX II), the sampling is performed asynchronously and the sample clock is independent of the symbol rate. At the highest required data rate

of 6.6 Msymbols/sec and the processing rate of 20 MHz for the Block V receiver, only about three samples per symbol are obtained.

Some analytical results for the phase-error variance of the analog DTTL were first derived in [2], where the input was an analog signal and symbol and midphase detection were performed with analog I&D filters. Later, the analysis was reworked [3], taking into account variations of the equivalent noise spectrum with respect to normalized phase error.

The interest here is in the loop response and performance of all-digital DTTLs, where digital symbol detection and digital midphase accumulation are used. There are two sampling scenarios: one is to sample the signal instantaneously, and the other is to obtain the sample by I&D sampling of the signal. The instantaneous sampling technique can be used when the sampling rate is significantly higher than the symbol rate. The I&D sampling technique should be used when the number of samples per symbol is small. If the received symbol waveform is a perfect square wave, the samples by instantaneous sampling all have equal amplitude. The samples by I&D sampling also have equal amplitude, except for the first sample of every symbol which has a different polarity from the symbol immediately preceding it. These changes in symbol polarity are referred to as the transition boundaries. The first sample after each transition boundary has a smaller amplitude than other samples due to integration across the transition boundary. The all-digital DTTL can operate on either type of sample. It is worthwhile noting at this time that when the received signal is filtered and instantaneously sampled, the process can be modeled to the first degree by I&D sampling of an ideal waveform. Thus, I&D sampling can be thought of as a tool to model the filtering operations in the receiver.

The components in the all-digital DTTL affected by the type of sampling are the symbol detector and the midphase accumulator. For instantaneous sampling, the symbol detector accumulates all samples in the current symbol epoch. The midphase detector accumulates all samples in the current transition-detection window. For I&D sampling, the problem is slightly different. In this case, even when a sample is in the current symbol epoch, most of its energy may be from the previous symbol epoch. Therefore, a more sophisticated rule is needed to determine whether a particular sample should be used for the detection of a particular symbol.

A reasonable criterion is to include a particular sample in the current symbol if more than half of its energy is from the current symbol. This criterion leads to a simple rule for the operation of the symbol and midphase detectors. The rule is as follows: the first sample after each symbol boundary should belong to the previous symbol if the time offset between the sample and the symbol boundary is less than half of the sampling interval; otherwise, the sample belongs to the current symbol. A sample mark is one-half of a sampling interval ahead of its respective sample time for I&D sampling, and is the respective sample time for instantaneous sampling. Thus, the rule can be restated: the symbol detector accumulates all samples with their sample marks in the current symbol epoch, and the midphase detector accumulates all samples with their sample marks in the current transition-detection window. Therefore, the DTTL with I&D sampling is similar to that with instantaneous sampling if the concept of a sample mark is used.

To simplify the mathematical analysis, the effects of unequal I&D sample amplitude immediately following transition boundaries are ignored, and instead equal amplitude for all I&D samples is assumed.

To illustrate the differences between analog and all-digital DTTLs, the noiseless case is considered first. Note that if the input is an analog signal, the midphase integrator can produce a nonzero error voltage no matter how small the phase error is. Thus, a correction voltage can be generated at every symbol transition whenever a phase error exists. Therefore, the analog DTTL has infinite resolution for phase detection.

In contrast, the all-digital DTTL has only finite resolution for phase detection. This is illustrated in the following example. Suppose that there is an even number of samples per symbol. When a symbol transition occurs, the digital midphase accumulator can produce a nonzero voltage only if the phase error causes sample slipping (assuming samples of equal amplitude). As long as the phase error stays within a range of values that avoids sample slipping, the loop always generates a no-error signal. This range of undetectable phase errors accounts for the finite resolution of the all-digital DTTL. The more samples per symbol that are used, the higher the achievable resolution, and the closer the all-digital DTTL is to its analog counterpart. A key question is the impact of the all-digital DTTL's finite resolution on the phase-error variance for few samples per symbol (say, four or five samples).

Another issue in an all-digital implementation is the effect of a noninteger number of samples per symbol. If the sampling clock is driven by the symbol-synchronization loop, the number of samples per symbol can be made an exact even integer, which reduces the self-noise generated

in the midphase accumulator (as discussed later). Under that sampling scenario, the sampling clock is constantly adapting as the data rate changes due to Doppler or other effects. One disadvantage of that scheme is that no fixed time base is available in the system. On the other hand, if the sampling clock is free-running and is derived from a fixed frequency standard, the sampling period is fixed, although the symbol rate may change. This may result in a noninteger number of samples per symbol. A model is derived in this article to analyze the performance of the DTTL where the sampling rate and the data rate are noncommensurate. Other issues such as the mean time to lose lock (MTLL), probability of symbol error, probability of losing lock, and error variance are also investigated via simulations. In Section II, a general analysis of the loop is presented in handling several scenarios. A discussion and comparison with simulation results are given in Section III, and the conclusion is given in Section IV.

II. Analysis

The performance of the all-digital data-transition tracking loop with noncoherent sampling is analyzed here. The block diagram of the all-digital DTTL is delineated in Fig. 1. The input $r(i)$ to the DTTL can be obtained by instantaneous sampling or by I&D sampling. For the Advanced Receiver II, the number of samples per symbol becomes small at high data rates, and therefore the I&D sampling technique is used. In the subsequent derivation, equal-amplitude samples are assumed.

Noncoherent sampling means that the sampling clock runs independently of the estimated symbol phase, i.e., the sampling time interval and the sampling time do not change with the estimated symbol phase. This is not an issue if there are many samples per symbol. The problem becomes complex as the number of samples per symbol decreases. The proposed Advanced Receiver II has about three to four samples per symbol at high data rates (the goal is 6.6 Msymbols per sec). Noncoherent sampling results in a noninteger number of samples per symbol. All of these factors affect the performance of the DTTL by changing its S-curve and by introducing self-noise. Considered here are the probability of loss of lock, the MTLL, the degradation of the symbol detection, and the phase-error variance. An approximate theory is presented for a first-order DTTL. The approach is to derive the S-curve and then solve the Fokker-Planck equation to get the density function of the phase error. The phase-error variance and the degradation of the symbol detection can be evaluated from the phase-error density function.

To illustrate the phenomenon of self-noise, a simple example is shown in Fig. 2, where there are five samples per symbol. Assumed are no thermal noise and perfect tracking at a particular moment. The output of the symbol-transition detector is not zero because it sums three samples from the first symbol and two samples from the second symbol (Fig. 2a). Notice that this situation occurs for every symbol interval as long as the loop maintains perfect tracking. The nonzero output of the loop filter will gradually drag the loop away from the perfect tracking condition until the polarity of the output of the symbol-transition detector changes (Fig. 2b). The loop filter cannot eliminate this type of self-noise. The problem is more complex if the number of samples per symbol is not an integer. In order to describe this phenomenon, three useful parameters are introduced here. Let β denote the number of samples per symbol, which may not be an integer, and α denote the offset of the first sample mark in a received symbol from the symbol boundary. By convention, α is normalized and is measured as a percentage of the sampling interval. If β is an integer, α remains constant; if β is not an integer, α varies from symbol to symbol. Let the received symbol be numbered 0, 1, 2, ..., and let the value of α at the first symbol be denoted as $\alpha_0 \equiv \gamma$, which is referred to as the initial sampling offset. The values of α at the subsequent symbols, namely, $\alpha_1, \alpha_2, \ldots$, can be computed from β and γ. The number of sample marks in a transition-detection window and the number of sample marks in a symbol-detection window are functions of α. Thus the output of the symbol detector and that of the transition detector fluctuate from symbol to symbol as α_i. This subject will be further discussed later.

Another important observation about the DTTL with noncoherent sampling is that there is inherent phase error due to finite samples per symbol. To illustrate this phenomenon, consider the example shown in Fig. 3, where every symbol contains four samples. As long as the estimated phase lies between t_1 and t_2, the error signal is always zero (or nearly zero if the received symbol does not have a perfect square waveform or if there are unequal-strength samples from I&D sampling), and the DTTL remains in tracking. However, unresolved phase ambiguity still exists within the interval from t_1 to t_2. Mathematically, this phase ambiguity can be explained by a step-like S-curve. This phenomenon might have little effect on symbol detection performance if straight accumulation is used to detect the symbols. However, if weighted accumulation is used to detect the symbols, the phase ambiguity can introduce misweighting and thus degrade performance. The symbol-error probability can be obtained by simulation.

Before proceeding to the mathematical analysis, examine the all-digital DTTL block diagram again in Fig. 1. The error-signal accumulator between the loop filter $F(z)$ and the multiplier performs an averaging function so that

the subsequent loop filter can operate at a slower speed. The loop bandwidth is determined primarily by the loop filter $F(z)$. Thus the presence of the accumulator is simply for hardware convenience. In the following analysis, the DTTL is considered without the error-signal accumulator.

A. Mathematical Model

Assuming that the carrier and subcarrier (if any) have been removed in an ideal fashion, the received waveform is given by

$$r(t) = \sqrt{S}\sum_k a_k\, p(t - kT) + n(t)$$

where S is the data power, $n(t)$ is white Gaussian noise with two-sided power spectral density $N_0/2$ W/Hz, $a_k = \pm 1$ represents the polarity of the kth symbol, and $p(t)$ is the square-wave function having value 1 for $0 \le t < T$ and having value 0 elsewhere. With I&D sampling, the ith sample can be expressed as

$$r(i) = \sqrt{S}a_k + n(i) \tag{1}$$

where it is assumed that the ith sample is derived from the kth symbol, $n(i)$ is a zero-mean Gaussian random variable with variance $\sigma^2 = N_0/(2T_s)$, and T_s is the sampling interval. Note that equal sample strength is assumed in Eq. (1).

Let the phase error λ (in cycles) be defined as

$$\lambda = \frac{\theta - \hat{\theta}}{2\pi}$$

where θ is the actual received symbol phase and $\hat{\theta}$ is the estimated symbol phase. Note that λ should have a value between -0.5 and 0.5. The error signal is affected by the locations of samples within their respective received symbols. In order to quantify this effect, a set of twelve Δ functions is defined, six for the $\lambda \ge 0$ case and six for the $\lambda < 0$ case. They are the numbers of sample marks contained in their respective intervals defined in Fig. 4(a). The output of the inphase accumulator $x(k)$ and the output of the midphase accumulator $y(k)$ can be expressed in terms of the Δ functions. If $\lambda \ge 0$, then

$$x(k) = \sqrt{S}(\Delta_1 a_k + \Delta_2 a_{k+1}) + n_1(k) + n_2(k) + n_3(k)$$

$$x(k+1) = \sqrt{S}(\Delta_3 a_{k+1} + \Delta_4 a_{k+2}) + n_4(k) + n_5(k) + n_6(k)$$

and

$$y(k) = \sqrt{S}(\Delta_5 a_k + \Delta_6 a_{k+1}) + n_2(k) + n_3(k) + n_4(k) \tag{2}$$

where $n_j(k)$, $1 \le j \le 6$ are zero-mean Gaussian random variables with their respective variances $(\Delta_1 - \Delta_5)\sigma^2$, $\Delta_5\sigma^2$, $\Delta_2\sigma^2$, $(\Delta_6 - \Delta_2)\sigma^2$, $(\Delta_3 + \Delta_2 - \Delta_6)\sigma^2$, and $\Delta_4\sigma^2$.

The Δ functions are computed using the following equations:

$$\Delta_1 = \lfloor \beta - \alpha \rfloor - \lfloor \lambda\beta - \alpha \rfloor$$

$$\Delta_2 = \lfloor (1+\lambda)\beta - \alpha \rfloor - \lfloor \beta - \alpha \rfloor$$

$$\Delta_3 = \lfloor 2\beta - \alpha \rfloor - \lfloor (1+\lambda)\beta - \alpha \rfloor$$

$$\Delta_4 = \lfloor (2+\lambda)\beta - \alpha \rfloor - \lfloor 2\beta - \alpha \rfloor \tag{3}$$

$$\Delta_5 = \begin{cases} \lfloor \beta - \alpha \rfloor - \lfloor (1+\lambda-(W/2))\beta - \alpha \rfloor & \text{if } W/2 > 1+\lambda \\ 0 & \text{if } W/2 < 1+\lambda \end{cases}$$

$$\Delta_6 = \begin{cases} \lfloor (1+\lambda+(W/2))\beta - \alpha \rfloor - \lfloor \beta - \alpha \rfloor & \text{if } W/2 > 1+\lambda \\ \lfloor (1+\lambda+(W/2))\beta - \alpha \rfloor - \lfloor (1+\lambda-(W/2))\beta - \alpha \rfloor & \text{if } W/2 < 1+\lambda \end{cases}$$

if $\lambda > 0$, and

$$\Delta_1' = \lfloor (1+\lambda)\beta - \alpha \rfloor + 1$$

$$\Delta_2' = \begin{cases} \lfloor -\lambda\beta + \alpha \rfloor & \text{if } -\lambda\beta + \alpha \text{ is not an integer} \\ \lfloor -\lambda\beta + \alpha \rfloor + 1 & \text{if } -\lambda\beta + \alpha \text{ is an integer} \end{cases}$$

$$\Delta_3' = \lfloor (2+\lambda)\beta - \alpha \rfloor - \lfloor \beta - \alpha \rfloor$$

$$\Delta_4' = \lfloor \beta - \alpha \rfloor - \lfloor (1+\lambda)\beta - \alpha \rfloor \tag{4}$$

$$\Delta_5' = \begin{cases} \lfloor \beta - \alpha \rfloor - \lfloor (1+\lambda-(W/2))\beta - \alpha \rfloor & \text{if } W/2 > -\lambda \\ \lfloor (1+\lambda+(W/2))\beta - \alpha \rfloor - \lfloor (1+\lambda-(W/2))\beta - \alpha \rfloor & \text{if } W/2 < -\lambda \end{cases}$$

$$\Delta_6' = \begin{cases} \lfloor (1+\lambda+(W/2))\beta - \alpha \rfloor - \lfloor \beta - \alpha \rfloor & \text{if } W/2 > -\lambda \\ 0 & \text{if } W/2 < -\lambda \end{cases}$$

if $\lambda < 0$, where $\lfloor y \rfloor$ is the greatest integer strictly less than y.

In the above equations, W is the width of the transition-detection window. The derivations of the twelve Δ functions are similar. Two examples are given here, Δ_2 and Δ_3'. To derive Δ_2, the beginning of the kth received symbol is used as the reference point. The number of sample marks in the kth received symbol is $\lfloor \beta - \alpha \rfloor$. The number of sample marks from the beginning of the kth received symbol to the end of the kth estimated symbol is $\lfloor (1+\lambda)\beta - \alpha \rfloor$. Equation (3) follows by observing that the number of sample marks from the end of the kth received symbol to the end of the kth estimated symbol is Δ_2. To derive Δ_3', the beginning of the kth received symbol is also used as the reference point. The number of sample marks in the kth received symbol is $\lfloor \beta - \alpha \rfloor$. The number of sample marks from the beginning of the kth received symbol to the end of the $(k+1)$th estimated symbol is $\lfloor (2+\lambda)\beta - \alpha \rfloor$. Equation (4) follows by observing that the number of sample marks from the end of the kth received symbol to the end of the $(k+1)$th estimated symbol is Δ_3'.

The error signal $e(k)$ is given by

$$e(k) = z(k)y(k)$$

The conditional S-curve is defined by

$$g(\lambda|\alpha) = E_{n,s}\{e(k)|\lambda, \alpha\}$$

where $E_{n,s}$ represents the conditional expectation on λ with respect to the noise and the signal. Following similar mathematical manipulation as in [2],

$$\frac{4E\{e(k)|\lambda \geq 0,\alpha\}}{\beta\sqrt{S}} = \frac{\Delta_6}{\beta}\left\{\operatorname{erf}\left(\sqrt{(\Delta_3+\Delta_4)E_s/\beta}\right) + \operatorname{erf}\left((\Delta_3-\Delta_4)\sqrt{E_s/(\beta(\Delta_3+\Delta_4))}\right)\right\}$$

$$- \frac{\Delta_5+\Delta_6}{\beta}\operatorname{erf}\left(\sqrt{(\Delta_1+\Delta_2)E_s/\beta}\right)$$

$$- \frac{\Delta_5-\Delta_6}{\beta}\operatorname{erf}\left((\Delta_1-\Delta_2)\sqrt{E_s/(\beta(\Delta_1+\Delta_2))}\right)$$

$$+ \frac{\Delta_6-\Delta_2}{\sqrt{\pi\beta(\Delta_3+\Delta_4)E_s}}\left\{\exp\left(-\frac{\Delta_3+\Delta_4}{\beta}E_s\right) + \exp\left(-\frac{(\Delta_3-\Delta_4)^2}{(\Delta_3+\Delta_4)\beta}E_s\right)\right\}$$

$$- \frac{\Delta_2+\Delta_5}{\sqrt{\pi\beta(\Delta_1+\Delta_2)E_s}}\left\{\exp\left(-\frac{\Delta_1+\Delta_2}{\beta}E_s\right) + \exp\left(-\frac{(\Delta_1-\Delta_2)^2}{(\Delta_1+\Delta_2)\beta}E_s\right)\right\}$$

where E_s is the symbol energy-to-noise ratio, namely,

$$E_s = \frac{ST}{N_0}$$

Using the same approach yields a similar result for the $\lambda < 0$ case:

$$\frac{4E\{e(k)|\lambda < 0,\alpha\}}{\beta\sqrt{S}} = \frac{\Delta'_5+\Delta'_6}{\beta}\operatorname{erf}\left(\sqrt{(\Delta'_3+\Delta'_4)E_s\beta}\right)$$

$$+ \frac{\Delta'_5-\Delta'_6}{\beta}\operatorname{erf}\left((\Delta'_4-\Delta'_3)\sqrt{E_s/(\beta(\Delta'_3-\Delta'_4))}\right)$$

$$- \frac{\Delta'_5}{\beta}\left\{\operatorname{erf}\left(\sqrt{(\Delta'_1+\Delta'_2)E_s/\beta}\right) + \operatorname{erf}\left((\Delta'_1-\Delta'_2)\sqrt{E_s/(\beta(\Delta'_1+\Delta'_2))}\right)\right\}$$

$$+ \frac{\Delta'_4-\Delta'_6}{\sqrt{\pi\beta(\Delta'_3+\Delta'_4)E_s}}\left\{\exp\left(-\frac{\Delta'_3+\Delta'_4}{\beta}E_s\right) + \exp\left(-\frac{(\Delta'_3-\Delta'_4)^2}{(\Delta'_3+\Delta'_4)\beta}E_s\right)\right\}$$

$$- \frac{\Delta'_5+\Delta'_4}{\sqrt{\pi\beta(\Delta'_1+\Delta'_2)E_s}}\left\{\exp\left(-\frac{\Delta'_1+\Delta'_2}{\beta}E_s\right) + \exp\left(-\frac{(\Delta'_1-\Delta'_2)^2}{(\Delta'_1+\Delta'_2)\beta}E_s\right)\right\}$$

Observe that $g(\lambda|\alpha)$ is the (unconditional) S-curve if α is a constant. If α changes rapidly from symbol to symbol, the loop filter will smooth its effect on the error signal. Therefore, the S-curve is obtained by averaging the above equations over a certain set of values of α, which is determined by the initial sampling offset and the number of samples per symbol. This problem is addressed in the subsequent discussion.

If β is an integer, the value of α remains constant from symbol to symbol, namely, $\alpha_i = \gamma$ for all i. For this case, the S-curve can be determined for a given γ. When γ is 0.5, the S-curve is centered; otherwise, the S-curve is biased slightly to one side. The phase error is certainly biased if the S-curve is biased. If β is an odd integer, the error signal is not zero when the phase error is zero. This is a source of self-noise, as discussed before.

Next, consider the effect of a noninteger number of samples per symbol on the S-curve. To illustrate the concept, assume that $\beta = 4.1$. Suppose that the initial sampling offset γ is 0.7. Clearly, $\alpha_0 = \gamma = 0.7$, $\alpha_1 = 0.6$, $\alpha_2 = 0.5$, $\alpha_3 = 0.4$, $\alpha_4 = 0.3$, $\alpha_5 = 0.2$, $\alpha_6 = 0.1$, $\alpha_7 = 0$, $\alpha_8 = 0.9$, $\alpha_9 = 0.8$, $\alpha_{10} = 0.7$, and so on. Consider a system with a normalized symbol rate of 1 Hz and a one-sided loop filter bandwidth of 0.05 Hz. The error-signal fluctuation due to variation of α is averaged by the loop filter in the same way as the fluctuation due to thermal noise. Therefore, the S-curve is obtained by averaging the error signal with respect to noise and all possible values of α. For the example given here, the set of values for α is $\{0, 0.1, 0.2, 0.3, 0.4, 0.5, 0.6, 0.7, 0.8, 0.9\}$. Figure 5 shows the conditional S-curve for the $\beta = 4.1$ case with $\alpha = 0.5$. Figure 6 shows the unconditional S-curve for the $\beta = 4.1$ case after averaging over values of α belonging to the set $\{0, 0.1, 0.2, 0.3, 0.4, 0.5, 0.6, 0.7, 0.8, 0.9\}$. There is a phase ambiguity area in the conditional S-curve in Fig. 5, i.e, zero error signal for nonzero phase error. The phase ambiguity is removed in the S-curve in Fig. 6 due to averaging over α. Notice the small bias of the S-curve due to the particular set of values for α.

Another example is the $\beta = 4.11$ case. The fractional part of β, i.e., 0.11, can be decomposed into the two components 0.1 and 0.01. Both components contribute to the values of α_i. For instance, if $\alpha_0 = \gamma = 0.7$, then $\alpha_1 = 0.59 = 0.7 - 0.1 - 0.01$, and $\alpha_2 = 0.48 = 0.7 - 0.2 - 0.02, \ldots$ and so on. The same loop bandwidth is assumed as before. The variation of α due to the component 0.1 changes quickly relative to the loop bandwidth, and the variation due to the component 0.01 changes slowly relative to the loop bandwidth. The S-curve is obtained approximately by averaging the error signal over all possible values of α due to the fast component. The initial sampling offset will drift slowly from time to time due to the slow component. The slow component does not affect the instantaneous S-curve, but it does affect the S-curve gradually by changing the initial sampling offset. Therefore, the slow component does contribute to the overall phase-error density function. Note that the conditional density function for the phase error can be obtained for any given initial sampling offset. The phase-error density function can then be derived by averaging the conditional density function over the initial sampling offset. The distribution function for the initial sampling offset can be assumed to be uniform between 0 and 1 or can be determined by simulation.

Partitioning the fractional part of β into slow and fast components can only be done approximately, and they are determined by the loop bandwidth. Let $\beta = n_\beta + f_{\beta,1} + f_{\beta,2}$, where n_β is the greatest integer less than or equal to β, $f_{\beta,1}$ is the fast component, and $f_{\beta,2}$ is the slow component. The choice of $f_{\beta,1}$ and $f_{\beta,2}$ is made solely by experience. In the following discussion, a criterion is provided for justifying the choice of $f_{\beta,1}$.

Let γ be the initial sampling offset. The set of values, denoted by $D_{\beta,\gamma}$ which $\{\alpha_i\}$ can take on, can be determined from γ and β using the following procedure: suppose that $f_{\beta,1}$ contains k digits after the decimal point (for instance, if $f_{\beta,1} = 0.15$, then $k = 2$). The basic incremental unit g_β is defined as

$$g_\beta = \frac{\mathrm{GCD}(10^k f_{\beta,1},\, 10^k)}{10^k}$$

where $\mathrm{GCD}(a, b)$ is the greatest common divisor between a and b. Then $D_{\beta,\gamma}$ is given by

$$D_{\beta,\gamma} = \left\{\gamma + m g_\beta | 0 \le m \le (1/g_\beta) - 1\right\}$$

For instance, if $\gamma = 0.1$ and $f_{\beta,1} = 0.15$, then $g_\beta = 0.05$, and $D_{\beta,0.1} = \{0.1 + 0.05m | 0 \le m \le 19\}$. In terms of $D_{\beta,\gamma}$, the S-curve is given by

$$g(\lambda|\gamma) = E_{\alpha \epsilon D_{\beta,\gamma}}\left\{g(\lambda|\alpha)\right\}$$

where the expectation is performed with respect to all values of α in $D_{\beta,\gamma}$, which are assumed equiprobable. Let the one-sided loop bandwidth be B_L and let the symbol rate be R. A valid choice for $f_{\beta,1}$ is to ensure that all values in $D_{\beta,\gamma}$ can occur in a $1/B_L$ time interval, i.e., to satisfy the following equation:

$$B_L \underline{\le} R g_\beta \qquad (5)$$

B. The Density Function and Variance of Phase Error

The steady-state Fokker-Planck Eq. (2) is given by

$$\frac{dP}{d\lambda}\Big\{A(\lambda|\gamma)P(\lambda|\gamma)\Big\} = \frac{1}{2}\frac{d^2}{d\lambda^2}\Big\{B(\lambda|\gamma)P(\lambda|\gamma)\Big\} \qquad (6)$$

In the above equation,

$$A(\lambda|\gamma) = -\frac{2B_L}{E_s N_0}\, g(\lambda|\gamma)$$

$$\beta(\lambda|\gamma) = \left(\frac{2B_L}{E_s N_0}\right)^2 S(0,\lambda|\gamma)$$

where $S(\omega,\lambda|\gamma)$ is the spectrum of the noise $n_\lambda(t)$ defined as

$$n_\lambda(t) = E_{n,s,\alpha\epsilon A_\beta,\gamma}\{e(k)e(k+m)|\lambda,\gamma\} - \Big(g(\lambda|\gamma)\Big)^2$$

The solution to Eq. (6) is of the form

$$P(\lambda|\gamma) = C\exp\left[\int_0^\lambda \frac{2A(y|\gamma) - \frac{dB(y|\gamma)}{dy}}{B(y|\gamma)}\, dy\right] \qquad (7)$$

In order to use the above equation, $S(0,\lambda|\gamma)$ must be found, which is a fairly complex task. In the subsequent derivation, it is assumed that $S(0,\lambda|\gamma) = WN_0T/4$. Thus Eq. (7) can be simplified to

$$P(\lambda|\gamma) = C\exp\left[-\frac{2E_s}{B_L RW}\int_0^\lambda g(y|\gamma);dy\right] \qquad (8)$$

The phase-error bias $E\{\lambda|\gamma\}$ is given by

$$E\{\lambda|\gamma\} = \int_{-1/2}^{1/2} \lambda P(\lambda|\gamma)\, d\lambda$$

The mean-square phase noise $\sigma^2(\lambda|\gamma)$ is given by

$$\sigma^2(\lambda|\gamma) = E\{\lambda^2|\gamma\} - (E\{\lambda|\gamma\})^2$$

The phase ambiguity phenomenon is a direct result of Eq. (8). Note that if $g(y|\gamma) = 0$ for $-\epsilon_1 < y < \epsilon_2$, the phase error is uniformly distributed between $-\epsilon_1$ and ϵ_2 when E_s approaches infinity.

III. Discussion and Numerical Results

Figure 7 shows the phase-error variance versus symbol signal-to-noise ratio (SNR) with an even integer number of samples per symbol. Notice that the phase-error variance approaches a limit as symbol SNR increases for the given number of samples per symbol. That limit of the phase-error variance is due to the phase ambiguity; thus it cannot be eliminated by increasing the symbol SNR. The phase ambiguity decreases as the number of samples per symbol increases.

Note that the phase ambiguity phenomenon may have an effect on the performance of weighted symbol detection. For illustration, Fig. 8 shows simulation results of the MTLL of the all-digital DTTL for various symbol SNRs and for 4 and 100 samples per symbol. The plot depicts normalized MTLL, which is the MTLL times the loop bandwidth. Notice that it usually takes a long time to simulate the MTLL performance; therefore, the loop operation was purposely simulated at a very low loop SNR (on the order of 3 to 9 dB) to guarantee loss of lock within a "practical" time period. It is clear that the four samples per symbol case ($\beta = 4$) loses lock more often than the $\beta = 100$ case. In the DSN, the symbol loop SNR is so high that the loop is expected to maintain lock over a whole track. It is still expected that the MTLL for the $\beta = 4$ case will be less than for the $\beta = 100$ case, but both of these will be large enough that lock is maintained over a whole track.

In a practical communication system, Doppler and Doppler rate are present due to the relative motion between transmitter and receiver. The effect of the Earth Doppler rate on a symbol rate of 6.6 Msymbols/sec is about 1 mHz/sec, which is enough to guarantee that the number of samples per symbol will not remain an exact integer for long. Consider a scenario designed for $\beta = 4$ samples per symbol, but due to Doppler rate, the actual number of samples per symbol is $\beta = 4.0000001$. In this scenario, the basic incremental unit is $g_\beta = 10^{-7}$. When the DTTL is operating with a 1-mHz-loop bandwidth, the time constant of the loop is about 1000 sec or 6.6 Gsymbols at a symbol rate of 6.6 Msymbols/sec. Since the loop is effectively averaging over all those symbols, the effect of the 10^{-7} basic incremental unit will be enough to smooth the composite S-curve as discussed earlier. This is because with a time constant of 1000 sec, Rg_β/B_L = 6.6 Gsymbols $\times 10^{-7} = 660 \gg 1$ (Eq. 5). This effectively smooths the S-curve so that the digital loop behaves like its equivalent analog counterpart. For a loop time constant of 1 sec (1-Hz loop bandwidth), $Rg_\beta/B_L = 0.66$. However, with a time constant of 0.2 sec (5-Hz loop bandwidth),

$Rg_\beta/B_L = 0.132$; therefore, self-noise might become considerable. But that case would still exhibit less self-noise than the exact four samples per symbol scenario. So overall, the Doppler rate helps in reducing the self-noise. Depending on the actual parameters, the self-noise degradation might become negligible. More simulations with Doppler rates are planned to verify this concept.

IV. Conclusion

The all-digital DTTL with coherent or noncoherent sampling is analyzed in this article. Two sampling schemes are considered, i.e., instantaneous sampling and I&D sampling. The theory presented here is valid for both sampling schemes. The effects of few samples per symbol and of noncommensurate sampling rates and symbol rates are addressed and analyzed. The phase ambiguity problem due to a small number of samples per symbol is illustrated, and it is shown that the phase ambiguity can be alleviated when there is a noninteger number of samples per symbol and the loop filter has appropriate bandwidth. A closed-form expression for the S-curve is derived for any number of samples per symbol. Finally, the interplay between the loop bandwidth and the number of samples per symbol in the reduction of self-noise is shown.

Acknowledgments

The authors would like to thank Joseph Statman, Dr. Ted Peng, Dr. William Hurd, Dr. Kurt Ware, and especially Dr. Brooks Thomas for bringing the "filling in" viewpoint to their attention.

References

[1] D. H. Brown and W. J. Hurd, "DSN Advanced Receiver: Breadboard Description and Test Results," *TDA Progress Report 42-89*, vol. January–March 1987, Jet Propulsion Laboratory, Pasadena, California, pp. 48–66, May 15, 1987.

[2] W. C. Lindsey and T. O. Anderson, "Digital-Data Transition Tracking Loop," *International Telemetry Conference*, Los Angeles, California, pp. 259–271, October 8–10, 1968.

[3] M. K. Simon, "An Analysis of the Steady-State Phase Noise Performance of a Digital Data-Transition Tracking Loop," *Jet Propulsion Laboratory Space Programs Summary 37-55*, vol. III, Jet Propulsion Laboratory, Pasadena, California, pp. 54–62, January 31, 1969.

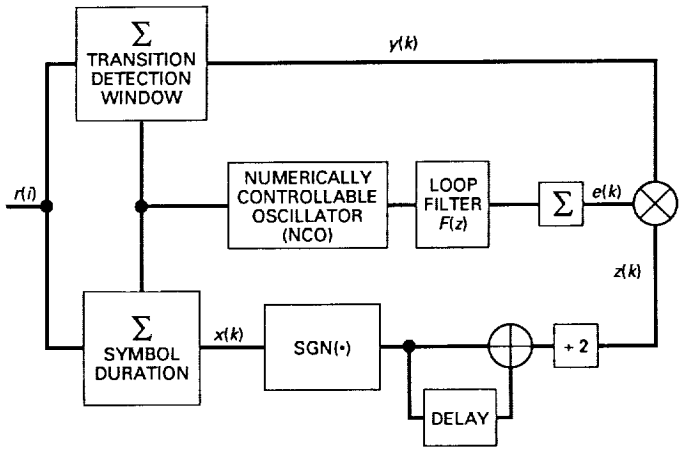

Fig. 1. Block diagram of the all-digital DTTL.

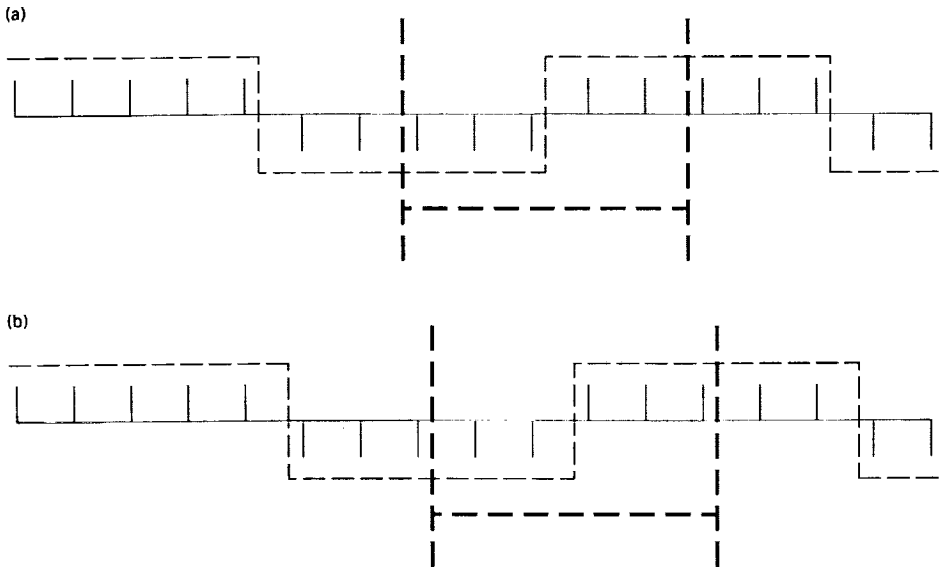

Fig. 2. Effect of odd number of samples per symbol: (a) local reference waveform is ahead of the received waveform, (b) local reference waveform is behind the received waveform.

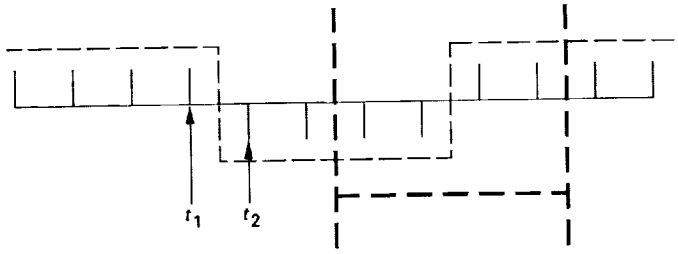

Fig. 3. The phase ambiguity phenomenon.

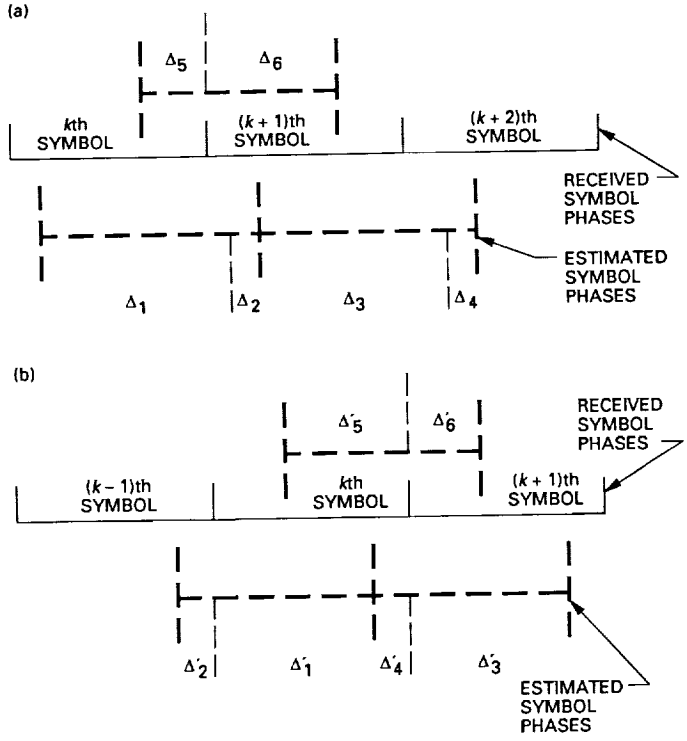

Fig. 4. The Δ functions: (a) $\lambda < 0$, (b) $\lambda \geq 0$.

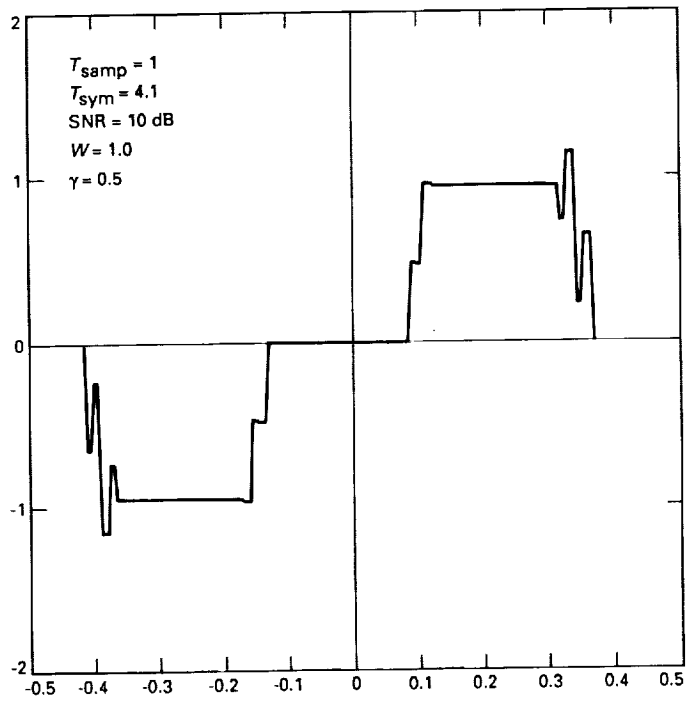

Fig. 5. Conditional S-curve for the $\beta = 4.1$ case.

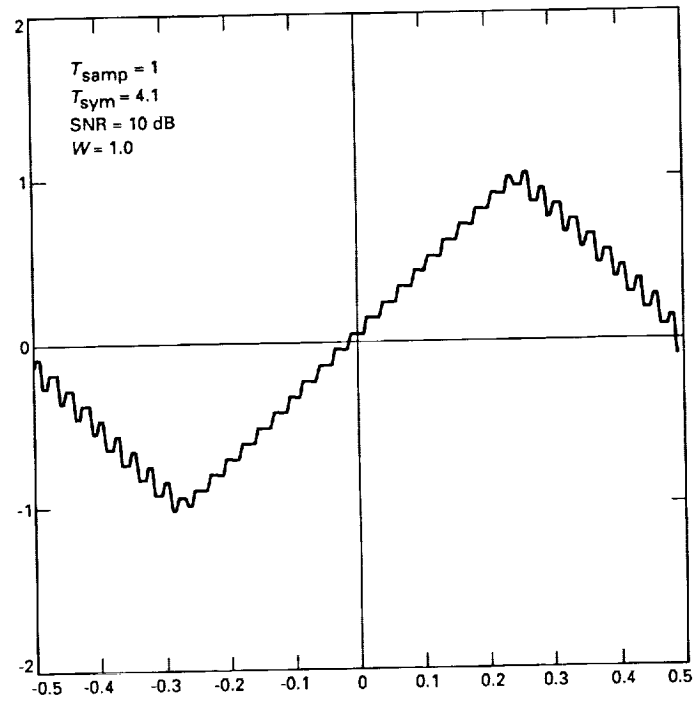

Fig. 6. S-curve for the $\beta = 4.1$ case by averaging over α belonging to the set $\{ 0, 0.1, 0.2, 0.3, 0.4, 0.5, 0.6, 0.7, 0.8, 0.9 \}$.

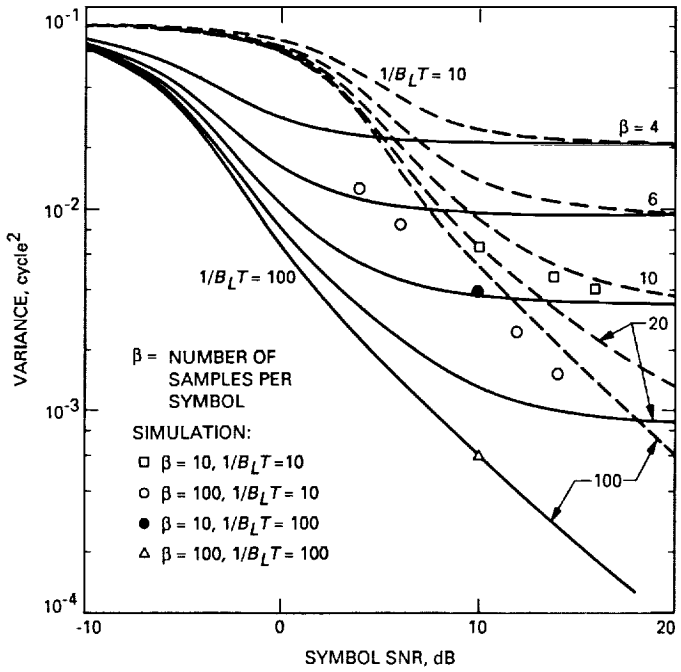

Fig. 7. Phase-error variance versus symbol SNR with even-integer number of samples per symbol.

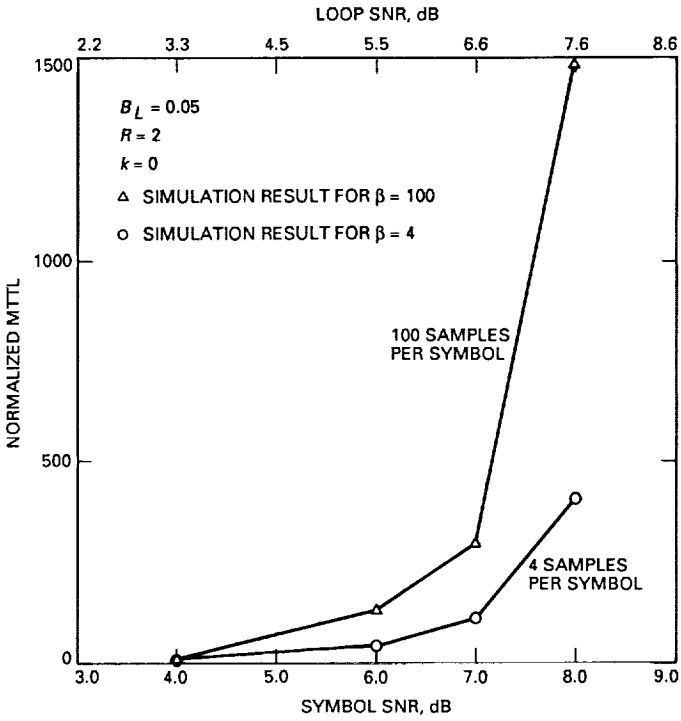

Fig. 8. Mean time to lose lock of all-digital DTTL versus symbol SNR for 4 and 100 samples per symbol.